

# Calculations of the $\beta$ -decay half-lives of neutron-deficient nuclei<sup>\*</sup>

Wenjin Tan(谭文金)<sup>1;1)</sup> Dongdong Ni(倪冬冬)<sup>1;4;2)</sup> Zhongzhou Ren(任中洲)<sup>1,2,3;3)</sup>

<sup>1</sup> Department of Physics, Nanjing University, Nanjing 210093, China

<sup>2</sup> Center of Theoretical Nuclear Physics, National Laboratory of Heavy-Ion Accelerator, Lanzhou 730000, China

<sup>3</sup> Kavli Institute for Theoretical Physics China, Beijing 100190, China

<sup>4</sup> Macao Univ Sci & Technol, Space Sci Inst, Macau, Peoples R China

**Abstract:** In this work,  $\beta^+$ /EC decays of some medium-mass nuclei are investigated within the extended quasiparticle random-phase approximation (QRPA), where neutron-neutron, proton-proton and neutron-proton (np) pairing correlations are taken into consideration in the specialized Hartree-Fock-Bogoliubov (HFB) transformation. In addition to the pairing interaction, the Brückner  $G$ -matrix obtained with the charge-dependent Bonn nucleon-nucleon force is used for the residual particle-particle and particle-hole interactions. Calculations are performed for even-even proton-rich isotopes ranging from  $Z=24$  to  $Z=34$ . It is found that the np pairing interaction plays a significant role in  $\beta$ -decay for some nuclei far from stability. Compared with other theoretical calculations, our calculations show good agreement with the available experimental data. Predictions of  $\beta$ -decay half-lives for some very neutron-deficient nuclei are made for reference.

**Keywords:** proton-rich nuclei,  $\beta^+$ /EC decay, quasiparticle random-phase approximation, neutron-proton pairing

**PACS:** 23.40.-s, 21.10.Tg, 23.60.+e, 21.60.Jz **DOI:** 10.1088/1674-1137/41/5/054103

## 1 Introduction

The neutron or proton drip line defines one of the limits of nuclear stability, and many nuclei lying between this line and the  $\beta$ -stable line are generally unstable against  $\beta$ -decay, with a natural tendency for a neutron to convert into a proton or vice versa.  $\beta$ -decay is of the most important decay channels of the unstable nuclei [1–4], and the properties of  $\beta$ -decay are useful to understand nuclear structure [5–7].

The properties of  $\beta$ -decay for nuclei far from the  $\beta$ -stable line have been measured by radioactive nuclear beam facilities over the last decade. Some updated data about  $\beta$ -decay half-lives have been measured with a higher degree of accuracy and some have been detected for the first time [8–11]. Along with the enhancement of the experimental facilities and the improvement of the sensitivity of experimental devices, it is expected that new  $\beta$ -decays of unstable nuclei approaching the proton drip line will be measured in the future. Experimental studies [12–14] of nuclei far from the  $\beta$ -stable line have made abundant progress and lots of  $\beta^+$ /EC-decay data have been accumulated. To accurately reproduce avail-

able experimental data and to reliably predict the half-lives of  $\beta^+$ /EC-decay of some unknown unstable nuclei is a stringent challenge, but also a good opportunity, for theorists.

Various theoretical models have been developed to describe nuclear  $\beta$ -decay. The phenomenological analysis [15–18], which is known for its simplicity, including gross theory [15] and semi-gross theory [17], can interpret some key properties of decay phenomena satisfactorily. The shell model [19–22] is based on the mean field theory, where nuclear structure properties can be reproduced using effective interactions and abundant basis states. The shell model calculations can be accurate for light nuclei, but are difficult for medium or heavy nuclei, because a very large shell-model basis is needed for calculation. Finally, the proton-neutron quasiparticle random phase approximation (pnQRPA) can describe the structure of nuclear collective excitations [23–26], and has been widely used for medium mass and even heavy nuclei. One can notice that the calculations of  $\beta$ -decay half-lives proceed from simple pictures to complex systems, and from empirical mean-field potentials to self-consistent models.

Received 10 November 2016, Revised 20 December 2016

<sup>\*</sup> Supported by National Nature Science Foundation of China (11535004, 11375086, 11120101005, 11175085 and 11235001), 973 Nation Major State Basic Research and Development of China (2013CB834400) and Science and Technology Development Fund of Macau (020/2014/A1 and 039/2013/A2)

1) E-mail: tanwenjin@smail.nju.edu.cn

2) E-mail: dongdongnick@gmail.com

3) E-mail: zren@nju.edu.cn

©2017 Chinese Physical Society and the Institute of High Energy Physics of the Chinese Academy of Sciences and the Institute of Modern Physics of the Chinese Academy of Sciences and IOP Publishing Ltd

The purpose of this work is to present detailed calculations of  $\beta^+$ /EC-decay half-lives for even-even proton-rich medium nuclei based on the extended QRPA with np pairing. Compared with some other pnQRPA calculations of  $\beta$ -decay half-lives [27, 28], there are two main differences. First, the two-body interactions matrix is obtained with charge-dependent Bonn forces instead of the simple  $\delta$ -form or separable schematic interactions. Second, besides proton-proton and neutron-neutron pairing correlations, neutron-proton (np) pairing correlations are taken into consideration in the HFB calculation. As a result, one has to solve the extended QRPA matrix equations where pp, nn, and np residual interactions are taken into account. Moreover, numerical calculations require good stability for program codes with np pairing, and the computation time increases greatly because the dimensions of the QRPA matrix equations become large. In this article, we pay special attention to the effect of np pairing for  $\beta^+$ /EC-decay half-lives. The  $T = 1$ ,  $J = 0$  pairing interaction has been introduced into the HFB equation, and meanwhile the  $T = 0$ ,  $J = 1$  pairing interaction effect has been considered by renormalizing the np pairing gap to the empirical pairing gap. This paper is organized as follows. In Section 2, we briefly present the formulas for the evaluation of  $\beta$ -decay half-lives in the framework of the extended QRPA. In Section 3, the residual interactions are explained in detail, together with the sensitivity of the results to some quantities used in the calculations, and the theoretical results of our calculations compared with the available experimental data and other theoretical results are also shown. A summary is given in Section 4.

## 2 Theoretical framework

The process of  $\beta$ -decay generally occurs from an initial ground state  $i$  of the parent nucleus to some possible final states  $f$  in the daughter nucleus. The  $\beta$ -decay half-life for allowed Gamow-Teller decay is given by the following formula [29, 30]:

$$T_{1/2} = \frac{2\pi^3 \hbar^7 \ln 2}{g_A^2 m_e^5 c^4} \left[ \sum_{0 < E_f < Q_\beta} B(1_m^+, E_f) f(Z, R, E_0) \right]^{-1}, \quad (1)$$

where  $g_A$  is the weak interaction coupling constant,  $E_0$  is the maximum energy of the  $\beta$  particle and  $E_f$  is the excitation energy of the  $m$ th excited  $|1^+\rangle$  state in the daughter nucleus. In this work, we set the constant  $g_A$  to 1 rather than its actual value of 1.26, to account for the near-universal quenching of iso-vector spin matrix elements in nuclei [31]. The quantity  $B(1_m^+, E_f)$  is the so-called reduced transition probability for the  $m$ th excited

$|1^+\rangle$  state. Its expression is as follows:

$$B(1_m^+, E_f) = \frac{1}{2J_i + 1} \left| \left\langle 1_m^+ \left\| \sum_k \tau_\pm(k) \sigma(k) \right\| 0^+ \right\rangle \right|^2, \quad (2)$$

where  $\tau_\pm$  is the isospin raising/lowering operator,  $\tau_- |p\rangle = |n\rangle$  and  $\tau_+ |n\rangle = |p\rangle$ ,  $\sigma$  is the Pauli spin matrix, and the sum is taken over all nucleons in the nucleus. The phase-space factor  $f(Z, R, E_0)$  is also called the integrated Fermi function describing the size of the phase space. It incorporates infinite nuclear size and Coulomb screening corrections. The  $f$ -values are evaluated with the following formula [29, 30]:

$$f(Z, R, E_0) = \int_1^{E_0} dE (E_0 - E)^2 E \sqrt{E^2 - 1} F(Z, R, E), \quad (3)$$

where  $E$  is the total energy of the  $\beta$  particle including its rest energy,  $Z$  and  $R$  are, respectively, the atomic number and the nuclear radius of the daughter nucleus and  $F(Z, R, E)$  is the Fermi function which accounts for the Coulomb interaction between the charged  $\beta$  particle and the residual daughter nucleus [30, 32]

We need to know the initial and final nuclear states,  $|0^+\rangle$  and  $|1_m^+\rangle$ , so as to evaluate the half-life. In our calculations, they are treated with the extended QRPA [33–36] introduced by Cheoun, Faessler et al. The formalism of the extended QRPA has been given in the works of Cheoun, Faessler et al, but for completeness we will briefly present the theoretical basis, which is of significance for this work. The first step of our calculations is to deal with the  $T = 1$ ,  $J = 0$  proton-proton, neutron-neutron and neutron-proton (np) pairing correlations using the HFB equations, which change the description picture from the simple single-particle mean-field to quasi-particle states for the decaying ground state. The quasi-particle states are made by an admixture of neutron and proton single-particle states. Then the particle-hole and particle-particle excitations are taken into account using the extended QRPA equations, which admix the pure quasiparticle states for the excitation states of residual daughter nuclei.

### 2.1 Hartree-Fock-Bogoliubov equations with np pairing

With the restrictions on spherical and time-reversal symmetry, the general HFB transformation is reduced to the following simple form [33, 34]:

$$\begin{pmatrix} b_1^\dagger \\ b_2^\dagger \\ b_{\bar{1}} \\ b_{\bar{2}} \end{pmatrix}_c = \begin{pmatrix} u_{1p} & u_{1n} & v_{1p} & v_{1n} \\ u_{2p} & u_{2n} & v_{2p} & v_{2n} \\ -v_{1p} & -v_{1n} & u_{1p} & u_{1n} \\ -v_{2p} & -v_{2n} & u_{2p} & u_{2n} \end{pmatrix}_c \begin{pmatrix} a_p^\dagger \\ a_n^\dagger \\ a_{\bar{p}} \\ a_{\bar{n}} \end{pmatrix}_c \quad (4)$$

where the subscript  $c$  stands for the single nucleon state of  $(n_c, l_c, j_c)$ . The operators  $b_{c\alpha'}^\dagger$  and  $b_{c\alpha'}$  are creation and annihilation operators of the quasiparticle in the state  $c$  with an isospin  $\alpha'$ . The operators  $a_{c\alpha}^\dagger$  and  $a_{c\alpha}$  are creation and annihilation operators of the nucleon in the state  $c$  with an isospin  $\alpha$ . In this article, a Greek letter always denotes the isospin of nucleons and this letter with a prime denotes the isospin of quasiparticles. The coefficients  $u$  and  $v$  are obtained by solving the HFB equation as follows [33–35]:

$$\begin{pmatrix} \epsilon_p - \lambda_p & 0 & \Delta_{p\bar{p}} & \Delta_{p\bar{n}} \\ 0 & \epsilon_n - \lambda_n & \Delta_{n\bar{p}} & \Delta_{n\bar{n}} \\ \Delta_{p\bar{p}} & \Delta_{p\bar{n}} & -\epsilon_p + \lambda_p & 0 \\ \Delta_{n\bar{p}} & \Delta_{n\bar{n}} & 0 & -\epsilon_n + \lambda_n \end{pmatrix}_c \begin{pmatrix} u_{\alpha'p} \\ u_{\alpha'n} \\ v_{\alpha'p} \\ v_{\alpha'n} \end{pmatrix}_c = E_{c\alpha'} \begin{pmatrix} u_{\alpha'p} \\ u_{\alpha'n} \\ v_{\alpha'p} \\ v_{\alpha'n} \end{pmatrix}_c \quad (5)$$

where  $\epsilon_{c\alpha}$  is the energy of the nucleon with isospin  $\alpha$  in state  $c$  and  $E_{c\alpha'}$  is the energy of the quasiparticle with isospin  $\alpha'$  in state  $c$ . Here, the single-particle energies are obtained by solving the Schrödinger equation with the Coulomb-corrected Woods-Saxon mean-field potential. If we ignore np pairing (i.e.  $\Delta_{n\bar{p}} = 0$ ), Equation (5) reduces to the usual BCS equation, naturally. The pairing gap  $\Delta_{c\alpha\bar{\epsilon}\beta}$  is expressed as [33–35]:

$$\begin{aligned} \Delta_{c\alpha\bar{\epsilon}\beta} &= -\frac{1}{2(2j_c + 1)^{1/2}} d_{\alpha\beta} \\ &\times \sum_e G(ccee, J=0, T=1)(2j_e + 1)^{1/2} \\ &\times (u_{e1\beta} v_{e1\alpha} + u_{e2\beta} v_{e2\alpha}), \quad \text{with } \alpha\beta = pp, nn, np \end{aligned} \quad (6)$$

In this expression,  $d_{\alpha\beta}$  is mainly used to renormalize the pairing potential gaps to the empirical pairing gaps.  $G$  are the two-body matrix elements, and they are evaluated based on the Brückner matrix with the charge-dependent Bonn nucleon-nucleon force and the Coulomb interaction. The detailed calculations are described in [36], as well as the parameters used in the calculations. The matrices of particle-particle interaction for the QRPA phonons are also evaluated using the same calculation procedure. Then the matrices of particle-hole interaction for the QRPA phonons are obtained from the matrices of particle-particle interaction by the Pandya transformation [33–35].

## 2.2 Extended QRPA equations with np pairing

As a result of neutron-proton (np) pairing correlations used in the HFB calculation, one has to solve the extended QRPA matrix equations with pp, nn, and np

residual interactions. The extended QRPA equation has the following form [33–35]:

$$\begin{pmatrix} A & B \\ -B & -A \end{pmatrix} \begin{pmatrix} X_j^m \\ Y_j^m \end{pmatrix} = \omega_j^m \begin{pmatrix} X_j^m \\ Y_j^m \end{pmatrix} \quad (7)$$

with

$$\begin{aligned} A &= \begin{pmatrix} A^{11,11} & A^{11,22} & A^{11,12} \\ A^{22,11} & A^{22,22} & A^{22,12} \\ A^{12,11} & A^{12,22} & A^{12,12} \end{pmatrix}, \\ B &= \begin{pmatrix} B^{11,11} & B^{11,22} & B^{11,12} \\ B^{22,11} & B^{22,22} & B^{22,12} \\ B^{12,11} & B^{12,22} & B^{12,12} \end{pmatrix} \end{aligned} \quad (8)$$

and

$$X_j^m = \begin{pmatrix} X_{(11)J}^m \\ X_{(22)J}^m \\ X_{(12)J}^m \end{pmatrix}, \quad Y_j^m = \begin{pmatrix} Y_{(11)J}^m \\ Y_{(22)J}^m \\ Y_{(12)J}^m \end{pmatrix}, \quad (9)$$

The details of the matrices  $A$  and  $B$  and the treatment of the particle-particle and particle-hole matrix elements can be found in Refs. [33–35]. The forward and backward-going amplitudes  $X$ ,  $Y$ , as well as the QRPA energies  $\omega$ , can be obtained by solving the extended QRPA Eq. (7).

Next, the reduced transition probability for the transition from the ground state  $|0_{g.s.}^+\rangle$  of an even-even nucleus to the  $m$ th one-phonon state  $|1^+\rangle$  of the nearby odd-odd nucleus is given by  $B(1_m^+, E_f) = |Z_\omega(m)|^2$ , with

$$\begin{aligned} Z_\omega(m) &= \sum_{a\alpha'b\beta'} [X_{(a\alpha'b\beta')1}^m u_{a\alpha'p} v_{b\beta'n} \\ &+ Y_{(a\alpha'b\beta')1}^m v_{a\alpha'p} u_{b\beta'n}] 2 \left\langle l_a \frac{1}{2} j_a \parallel \sigma \parallel l_b \frac{1}{2} j_b \right\rangle. \end{aligned} \quad (10)$$

In order to compute the excitation energy  $E_f$ , we take the sum of the lowest two quasiparticle energies  $(E_1 + E_2)_{\text{lowest}}$  obtained from Eq. (5) as the ground-state energy of the residual odd-odd nucleus. Hence the excitation energy of the  $m$ th state  $|1^+\rangle$  is given by  $E_f = \omega^m - (E_1 + E_2)_{\text{lowest}}$ . The reason why we choose the energy  $E_f$  instead of directly using the QRPA energy  $\omega_1^m$  is that the excitation energies have a considerable influence on the phase-space factor  $f(Z, R, E_0)$  in Equation (3) by the expression  $E_0 = Q_\beta - E_f$  [36].

## 3 Numerical results and discussion

The HFB equation (5) is iteratively solved until the pairing gaps are exactly equal to the empirical pairing gaps. In some articles [27] the empirical pairing gaps are simply taken as  $\Delta_{pp}$ ,  $\Delta_{nn} = 12.2/\sqrt{A}$  and  $\Delta_{np} = 20.0/A$ ,

respectively. However, here, the empirical pairing gaps  $\Delta_{pp}$ ,  $\Delta_{nn}$  and  $\Delta_{np}$  are extracted from the proton and neutron separation energies in the following way [37]:

$$\begin{aligned}\Delta_{pp} &= \frac{1}{4}(-1)^{Z+1}[S_p(A+1, Z+1) \\ &\quad - 2S_p(A, Z) + S_p(A-1, Z-1)], \\ \Delta_{nn} &= \frac{1}{4}(-1)^{A-Z+1}[S_n(A+1, Z) \\ &\quad - 2S_n(A, Z) + S_n(A-1, Z)], \\ \Delta_{np} &= \frac{1}{4}(-1)^A\{[S_n(A+2, Z+1) - S_n(A+1, Z+1)] \\ &\quad - 2[S_n(A+1, Z) - S_n(A, Z)] \\ &\quad + [S_n(A, Z-1) - S_n(A-1, Z-1)]\}.\end{aligned}\quad (11)$$

In the HFB calculation, the pairing parameters  $d_{pp}$ ,  $d_{nn}$  and  $d_{np}$  are used to renormalize the Brückner  $G$ -matrix elements to reproduce the empirical pairing gaps. The following two steps are taken. First, in the usual BCS equation, the parameters  $d_{pp}$  and  $d_{nn}$  are determined by fitting the lowest proton and neutron quasiparticle energies to the empirical pairing gaps  $\Delta_{pp}$  and  $\Delta_{nn}$ . Second, with the fixed  $d_{pp}$  and  $d_{nn}$  values, we adjust  $d_{np}$  to reproduce the empirical np pairing gap  $\Delta_{np}$ . That means the pairing parameter  $d_{np}$  is varied until the following condition is nearly satisfied [33]:

$$\Delta_{np} = (H_0 + E_1 + E_2) - (H'_0 + E'_1 + E'_2), \quad (12)$$

Table 1. Proton-proton (pp), neutron-neutron (nn) and neutron-proton (np) pairing parameters for the even-even Fe and Zn isotopes. These values are obtained by reproducing the empirical pairing gaps listed in the last column. The total ground-state energies calculated with and without np pairing are listed as well.

nucleus	$d_{pp}$	$d_{nn}$	$E_{total}/\text{MeV}$	$d_{np}$	$E'_{total}/\text{MeV}$	$(\Delta_{pp}, \Delta_{nn}, \Delta_{np})/\text{MeV}$
$^{46}\text{Fe}$	1.298	1.264	-783.914	2.264	-784.347	(1.582, 2.027, 0.432)
$^{48}\text{Fe}$	1.357	1.635	-849.316	2.392	-849.911	(1.675, 1.785, 0.595)
$^{50}\text{Fe}$	1.304	1.635	-909.491	2.547	-909.944	(1.509, 1.855, 0.453)
$^{56}\text{Zn}$	1.946	1.575	-993.771	2.264	-993.921	(1.350, 1.710, 0.147)
$^{58}\text{Zn}$	1.837	1.735	-1053.631	2.469	-1053.738	(1.227, 1.900, 0.107)
$^{60}\text{Zn}$	1.117	1.015	-1110.314	2.725	-1111.163	(1.635, 1.706, 0.849)
$^{62}\text{Zn}$	1.916	1.635	-1160.855	2.877	-1161.420	(1.369, 1.604, 0.608)

In Fig. 1, the variation of the calculated half-life as a function of the empirical pairing gap is shown for the  $\beta^+$ -decay of  $^{58}\text{Zn}$ . Minor changes in the calculated half-life are found as the empirical pairing gaps are varied, and it shows the weak dependence of the half-life on the pairing gap energy. This feature is in accordance with the other theoretical investigation [28].

The particle-hole interaction strength  $g_{ph}$  is determined in QRPA calculations by reproducing the position of Gamow-Teller giant resonances (GTGR) at a high excitation energy [29, 38], which is observed by (p, n) and (n, p) charge-exchange reactions. It is found that the value of  $g_{ph}$  can be reasonably set to a common value of 0.60 for medium-mass nuclei. In order to set

where  $H_0 + E_1 + E_2 (H'_0 + E'_1 + E'_2)$  is the sum of ground-state energy and the lowest two quasiparticle energies without (with) np pairing.

The results of the HFB calculations for Fe and Zn isotopes are displayed clearly in Table 1. The values of the strengths  $d_{pp}$ ,  $d_{nn}$  and  $d_{np}$  are obtained by reproducing the empirical gaps. These gaps are obtained from the relationship (11), where some nucleon separation energies are estimated by mass systematics [37] or theoretical extrapolation for some nuclei far from the  $\beta$ -stability line. The first column of Table 1 stands for the investigated nucleus. The second, third, and fourth columns display the values of the pairing parameters  $d_{pp}$ ,  $d_{nn}$  and the total ground-state energy calculated without np pairing. The fifth and sixth columns give the values for the parameter  $d_{np}$  and the total ground-state energy calculated with np pairing, while the empirical gaps  $\Delta_{pp}$ ,  $\Delta_{nn}$  and  $\Delta_{np}$  are listed in the last column. One can find from Table 1 that the  $d_{np}$  values are generally larger than the  $d_{pp}$  and  $d_{nn}$  values. The reason for this is that the  $T = 0, J = 1$  pairing contribution is compensated by enhancing the  $T = 1, J = 0$  pairing strength  $d_{np}$ . Comparing the fourth and sixth columns, one can also notice that the total ground-state energies calculated with np pairing ( $E'_{total}$ ) are generally lower than without np pairing ( $E_{total}$ ) for all nuclei listed in Table 1.

the particle-particle interaction strength  $g_{pp}$ , one needs to choose a physical quantity which is sensitive to the particle-particle interaction. In this work, the  $g_{pp}$  value is varied until the calculated  $\beta$ -decay half-lives gets close to the experimental one. It is found that our calculations work well when the value of  $g_{pp}$  is nearly equal to the half of the  $g_{ph}$  value.

The  $Q_\beta$  value not only affects the  $\beta$ -strength function, but also the evaluation of the phase-space factor, as shown in Eq. (1). In our calculations, the  $\beta$ -decay energy  $Q_\beta$  is set by experiments [37]. For some nuclei far from the  $\beta$ -stable line, the experimental data are still unknown and instead the theoretical values obtained by extrapolation are used. As the  $Q_\beta$  value of  $^{42}\text{Cr}$  is changed from

12.0 to 14.0 MeV, the calculated half-life is decreased by a factor of roughly 3.5. Also, we discuss the theoretical uncertainty resulting from the uncertainty in  $Q_\beta$  value. The  $Q_\beta$  value for  $^{60}\text{Ge}$  is currently taken as 12.18(0.28) MeV [37]. The uncertainty of 0.28 MeV brings an uncertainty of  $-1.8/+2.0$  ms for the calculated half-life, corresponding to an effect of about  $-12\%$  and  $+14\%$ . Similarly for  $^{64}\text{Se}$ , the  $Q_\beta$  value taken as 12.72(0.59) MeV leads to an uncertainty in the half-life of  $-7.6/+3.1$  ms, corresponding to an effect of about  $-27\%$  and  $+16\%$ .

In Table 2, the theoretical results of some very neutron-deficient nuclei are given. The first column in Table 2 stands for the investigated parent nucleus with proton excess. The second and third columns are, respectively, the calculated half-lives with and without np pairing. The comparisons with some available experimental data [14], the theoretical predictions of Möller et al. [39] based on the finite range droplet model (FRDM), and the  $Q_\beta$  values [37] are listed in the last three columns. It is found that both our calculations and the results of the FRDM are of the same order of magnitude as the available experimental data. An interesting phenomenon that comes from the numerical calculations is that the half-lives of the nuclei close to the  $\beta$ -stable line are obviously less accurate than those approaching the proton drip line. The  $Q_\beta$

value decreases with increasing neutron number, leading to an increase in the half-life.  $\beta$ -decay rates are the weighted strength with the phase space factor in the  $Q_\beta$  window. Moreover, the phase space factor  $f$  generally increases with the energy of the  $\beta$  particle and hence the

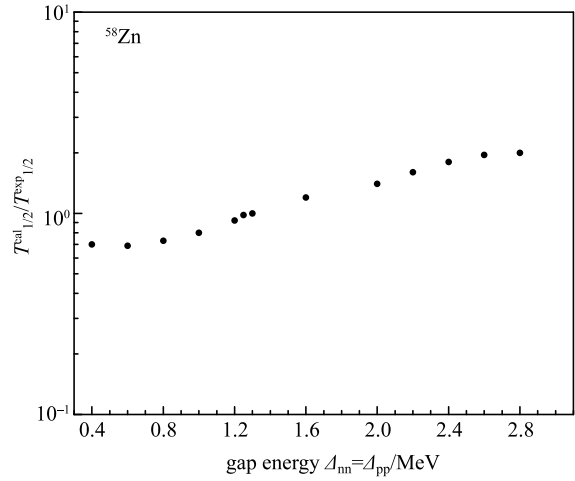


Fig. 1. Ratios of the calculated half-life to the experimental value [14, 37] versus the pairing gaps  $\Delta_{nn}=\Delta_{pp}$  for the  $\beta^+$ -decay of  $^{58}\text{Zn}$ , showing the weak sensitivity of the half-life to the pairing gap energy.

Table 2.  $\beta^+$ /EC-decay half-lives of some very neutron-deficient nuclei are predicted where the experimental data are still estimated values or not measured. Predictions of the work of Möller et al. [39] based on the finite-range droplet model (FRDM) are also given, and the  $Q_\beta$  values are listed as well. The half-life is given in seconds.

nucl.	$T_{1/2}$ (with np)	$T_{1/2}$ (without np)	$T_{1/2}^{\text{exp}}$ [14]	FRDM [39]	$Q_\beta/\text{MeV}$ [37]
$^{42}\text{Cr}$	0.0121	0.0134	0.0133	0.0450	13.860
$^{44}\text{Cr}$	0.0386	0.0560	0.0428	0.1186	10.480
$^{46}\text{Cr}$	0.3755	0.4040	0.2570	0.6710	7.6010
$^{46}\text{Fe}$	0.0106	0.0147	0.0130	0.0180	13.540
$^{48}\text{Fe}$	0.0344	0.0372	0.0453	0.0595	10.910
$^{50}\text{Fe}$	0.3006	0.3007	0.1550	0.5418	8.1400
$^{48}\text{Ni}$	0.0021	0.0046	0.0028	0.0054	15.610
$^{50}\text{Ni}$	0.0168	0.0185	0.0185	0.0168	12.880
$^{52}\text{Ni}$	0.0527	0.0565	0.0408	0.0767	10.520
$^{54}\text{Ni}$	0.2991	0.3291	0.1040	0.6459	8.7900
$^{56}\text{Zn}$	0.0210	0.0254	0.0300	0.0830	12.660
$^{58}\text{Zn}$	0.1620	0.1927	0.0860	0.5971	9.3700
$^{60}\text{Zn}$	60.290	268.30	142.80	>100	4.1700
$^{62}\text{Zn}$	31372	39372	33094	>100	1.6200
$^{60}\text{Ge}$	0.4240	0.4940	–	0.0820	12.180
$^{62}\text{Ge}$	0.1015	0.1256	0.1290	0.8684	10.090
$^{64}\text{Ge}$	665.62	752.20	63.700	80.880	4.5170
$^{66}\text{Ge}$	23144	25125	8136.0	>100	2.1170
$^{64}\text{Se}$	0.0200	0.0220	–	0.0971	12.720
$^{66}\text{Se}$	0.0650	0.0730	0.0330	0.6486	10.660
$^{68}\text{Se}$	17.680	17.690	35.500	42.320	4.7050
$^{70}\text{Se}$	3387.3	3388.4	2466.0	>100	2.4100

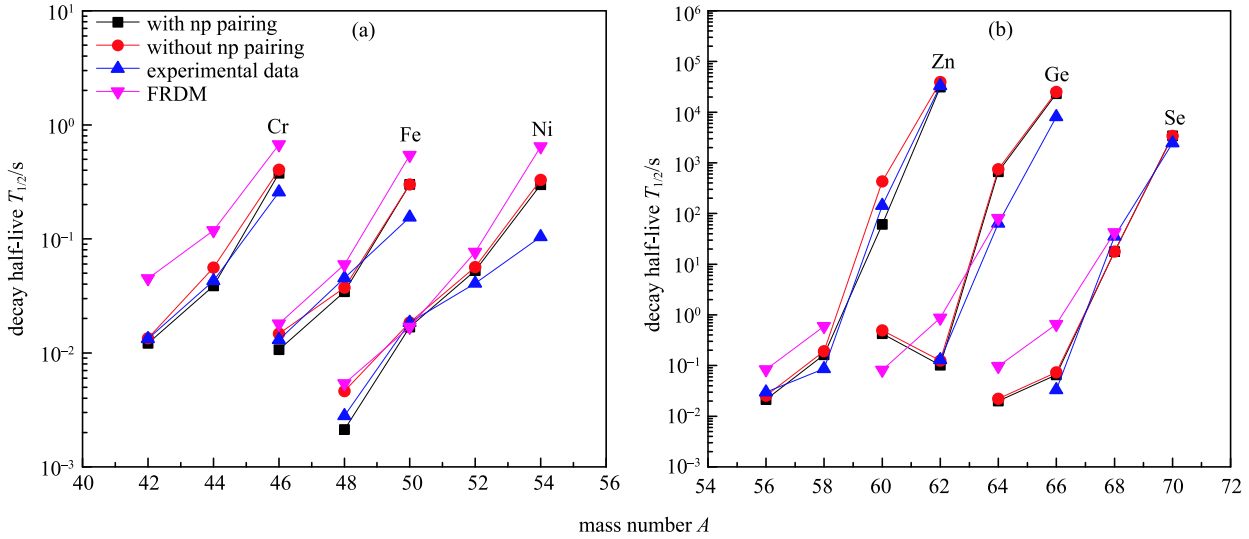


Fig. 2. (color online) Comparison of the calculated half-lives in this work with the experimental data for the neutron-deficient Cr-Fe-Ni-Zn-Ge-Se isotopes. The experimental  $\beta$ -decay half-lives of  $^{60}\text{Ge}$  and  $^{64}\text{Se}$  are still unknown in experiments. The theoretical results of Möller et al, in which they only give the half-life limits  $>100$  s for long-lived nuclei, are also given for comparison.

strengths located at low excitation energies have more contributions. For the isotopes close to the  $\beta$ -stable line with small  $Q_\beta$  values, some uncertainties, which could be ignored for exotic isotopes far from the  $\beta$ -stable line, may cause large variations of the theoretical results. So it is not surprising that there exist relatively large deviations from the experimental data near the  $\beta$ -stable line.

In Figure 2, the data of which come from Table 2, we show the comparison of half-lives of our calculations with the available experimental data and Möller's results for the neutron-deficient Cr-Fe-Ni-Zn-Ge-Se isotopes. Squares, circles, up-triangles and down-triangles respectively stand for the results of our work with np pairing, without np pairing, the available experimental data, and the theoretical results of Möller's work. Most of our calculations show good agreement with experimental data for short-lived nuclei far from the stability line. The calculated half-lives with np pairing are shorter than without np pairing and closer to the experimental data. This not only confirms the validity of our work but also allows us to make some predictions of  $\beta$ -decay half-lives for  $^{60}\text{Ge}$  and  $^{64}\text{Se}$ . One can expect that the np pairing plays a significant role in calculating the half-lives of short-lived neutron-deficient nuclei. This will give valuable guidance for  $\beta$ -decay of proton-rich nuclei far from  $\beta$ -stable line. One can also notice that the results of Möller et al. are generally longer than our calculations and the experimental data. There are abnormal cases for  $^{64}\text{Ge}$  and  $^{68}\text{Se}$ , where the FRDM results are smaller than

the present calculations and closer to the experimental data. The reason for this is that those two isotopes are located near the shape transition region. Nuclear deformations may have a large influence on their  $\beta$ -decay properties, which is beyond the scope of the present calculation.

## 4 Summary

In summary, we have presented in this article the calculations of  $\beta^+$ /EC-decay half-lives for even-even neutron-deficient medium-mass nuclei based on the extended QRPA with np pairing. The Brückner  $G$ -matrix with the charge-dependent Bonn nucleon-nucleon force is used for the residual particle-particle and particle-hole interactions along with the pairing interaction. To test the validity and application of this model, we also analyze the dependence of the calculated half-lives on some physical quantities used in calculations. The calculated results in Fig. 2 show agreement with the available experimental data. It is demonstrated that the np pairing correlations play a vital role, in particular for short-lived neutron-deficient nuclei. We also predict the half-lives of nuclei  $^{60}\text{Ge}$  and  $^{64}\text{Se}$ , for which experimental data are unclear or unmeasured. It is hoped that these predictions will be useful for future measurements. Besides, some large deviations from experimental data are seen for long-lived nuclei, and this is worth further investigation.

## References

- 1 H. Becquerel, Comptes Rendus, **122**: 420 (1896)
- 2 P. Ring, Prog. Part. Nucl. Phys., **37**: 193 (1996)
- 3 Samuel S. M. Wong, *Introductory Nuclear Physics*(Inc: prentice-hall, 1990), p.161–204
- 4 J. S. Lilley, *Nuclear Physics* (Chichester: Wiley, 2001), p.18–212
- 5 A. De Shalit, H. Feshbach, *Theoretical Nuclear Physics* (New York: Wiley, 1974), p.10–58
- 6 W. Pauli, Collected Scientific Papers, **2**: 1313 (1964)
- 7 E. Fermi, Zeitschrift für Physik, **88**: 161 (1934)
- 8 U. C. Bergmann et al. Nucl. Phys. A, **714**: 21 (2003)
- 9 S. Grevy et al, Phys. Lett. B, **594**: 252 (2004)
- 10 P. T. Hosmer et al, Phys. Rev. Lett., **94**: 112501 (2005)
- 11 P. F. Mantica et al, Phys. Rev. C, **77**: 014313 (2008)
- 12 L. J. Broussard, H. O. Back, M. S. Boswell et al, Phys. Rev. Lett., **112**: 212301 (2014)
- 13 M. R. Dunlop, C. E. Svensson, G. C. Ball et al, Phys. Rev. Lett., **116**: 172501 (2016)
- 14 G. Audi, F. G. Kondev, M. Wang, B. Pfeiffer, X. Su, J. Blachot, M. MacCormick, Chin. Phys. C, **36**: 1157 (2012)
- 15 K. Takahashi, M. Yamada, Prog. Theor. Phys., **41**: 1470 (1969)
- 16 B. Pfeiffer, K. L. Kratz, P. Möller, Prog. Nucl. Energy, **41**: 39 (2002)
- 17 H. Nakata, T. Tachibana, M. Yamada, Nucl. Phys. A, **625**: 521 (1997)
- 18 X. Zhang, Z. Z. Ren, Q. Zhi, Q. Zheng Q, J. Phys. G: Nucl. Part. Phys., **34**: 2611 (2007)
- 19 B. A. Brown, B. H. Wildenthal, At. Data Nucl. Data Tables, **33**: 347 (1985)
- 20 K. Muto, E. Bender, T. Oda T, Phys. Rev. C, **43**: 1487 (1991)
- 21 W. T. Chou, E. K. Warburton, B. A. Brown, Phys. Rev. C, **47**: 163 (1993)
- 22 G. Martínez-Pinedo, K. Langanke, Phys. Rev. Lett., **83**: 4502 (1999)
- 23 P. Möller P, J. Randrup, Nucl. Phys. A, **514**: 1 (1990)
- 24 A. Staudt, E. Bender, K. Muto, H. V. Klapdor-Kleingrothaus, At. Data Nucl. Data Tables, **44**: 79 (1990)
- 25 H. Homma, E. Bender, M. Hirsch, K. Muto, H. V. Klapdor-Kleingrothaus, T. Oda, Phys. Rev. C, **54**: 2972 (1996)
- 26 J. U. Nabi, H. V. Klapdor-Kleingrothaus, At. Data Nucl. Data Tables, **88**: 237 (2004)
- 27 D. D. Ni, Z. Z. Ren, J. Phys. G: Nucl. Part. Phys., **39**: 125105 (2012)
- 28 D. D. Ni, Z. Z. Ren, Q. J. Zhi, Sci. China Phys. Mech. Astron., **55**: 2397 (2012)
- 29 J. Suhonen, *From Nucleons to Nucleus: Concepts of Microscopic Nuclear Theory* (Berlin: Springer, 2007), p. 157–170
- 30 N. B. Gove, M. J. Martin, Nucl. Data Tables, **10**: 205 (1971)
- 31 J. Engel, M. Bender, J. Dobaczewski, W. Nazarewicz R. Surman, Phys. Rev. C, **60**: 014302 (1999)
- 32 W. R. Garrett, C. P. Bhalla, Z. Phys., **198**: 453 (1967)
- 33 M. K. Cheoun, A. Bobyk, A. Faessler, F. Simkovic, G. Teneva, Nucl. Phys. A, **561**: 74 (1993)
- 34 M. K. Cheoun, A. Bobyk, A. Faessler, F. Simkovic, G. Teneva, Nucl. Phys. A, **564**: 329 (1993)
- 35 M. K. Cheoun, A. Faessler, F. Simkovic, G. Teneva, A. Bobyk, Nucl. Phys. A, **587**: 301 (1995)
- 36 G. Pantis, F. Simkovic, J. D. Vergados, A. Faessler, Phys. Rev. C, **53**: 695 (1996)
- 37 M. Wang, G. Audi, A. H. Wapstra, F. G. Kondev, M. MacCormick, X. Xu, B. Pfeiffer, Chin.Phys. C, **36**: 1603 (2012)
- 38 P. Vogel, M. R. Zirnbauer, Phys. Rev. Lett., **57**: 3148 (1986)
- 39 P. Möller, J. R. Nix, K. L. Kratz, At. Data Nucl. Data Tables, **66**: 131 (1997)